A REAL-TIME ROLLING HORIZON CHANCE CONSTRAINED OPTIMIZATION MODEL FOR ENERGY HUB SCHEDULING

by

Weilin Hou

A Thesis Submitted in

Partial Fulfillment of the

Requirements for the Degree of

Master of Science

in Engineering

at

The University of Wisconsin-Milwaukee

May 2019

ABSTRACT

A REAL-TIME ROLLING HORIZON CHANCE CONSTRAINED OPTIMIZATION MODEL FOR ENERGY HUB SCHEDULING

by

Weilin Hou

The University of Wisconsin-Milwaukee, 2019
Under the Supervision of Professor Lingfeng Wang

With the increasing consumption of energy, it is of high significance to improve energy efficiency and realize optimal operation of the multi-energy system. Among the many energy system modeling methods, the concept of "energy hub (EH)" is an emerging one. However, the previous EH models only included one or a few of constituting components.

The construction of an energy hub model that integrates energy storage systems, photovoltaic (PV) components, a combined cooling heating and power (CCHP) system and electric vehicles (EVs) is explained in this thesis. The inclusion of the CCHP system helps to meet the energy demand and improve the mismatch of heat-to-electric ratio between the energy hub and the load. Additionally, vehicle-to-grid (V2G) technology is applied in this EH; that is, EVs are regarded not only as load demands but also as power suppliers.

The energy hub optimization scheduling problem is formulated as a multi-period stochastic problem with the minimum total energy cost as the objective. Compared to 24-hour day-ahead scheduling, rolling horizon optimization is used in the EH scheduling and shows its superiority. In

real-time rolling horizon scheduling, the optimization principle ensured that the result is optimized each moment, so it avoids energy waste caused by overbuying energy.

As part of electricity loads, EVs have certain influence on energy hub scheduling. However, due to the randomness of the driving patterns, it is still very difficult to perfectly predict the driving consumption and the charging availability of the EVs one day in advance. Chance constrained programming can hedge the risk of uncertainty for a big probability and drop the extreme case with a very low probability. By restricting the probability of chance constraints over a specific level, the influence of the uncertainty of electric vehicle charging behavior on energy hub scheduling can be reduced. Simulation results show that the energy hub optimization scheduling with chance constrained programming results in a less energy cost and it can make better use of time-varying PV energy as well as the peak-to-valley electricity price.

TABLE OF CONTENTS

LIST OF FIGURES

LIST OF TABLES

LIST OF ABBREVIATIONS

L_{el}	Electricity load of customer
L_h	Heating load
L_c	Cooling load
P_{pv}	PV output injected into the EH
W_{pv}	Weight matrix of PV scenarios
W_{ev}	Weight matrix of EV scenarios
P_{el}	Electricity exchange with power grid
P_{gas}	Buying gas from gas market
P_{gas}^{cchp}	Gas used in CCHP system from total gas
L_{cchp}^{e}	Electricity output from CCHP system
L_{cchp}^{h}	Heat output from CCHP system
L_{cchp}^{c}	Cool output from CCHP system
P_{gas}^{b}	Gas used in boiler from total gas
L_b	Heat output from boiler
P_r	Electricity used in refrigerator from total electricity
L_r	Cool output from refrigerator
S_h^{ch}	Heat injected into storage system per hour
S_c^{ch}	Cool injected into storage system per hour

L_{ev}^{ch}	Charging amount of electricity per hour per EV
L_{ev}^{m}	Charging amount of electricity per hour for all EVs when the EV amount is *m*
η_{cchp}	Power generation efficiency of the gas turbine
η_{loss}	Heat loss coefficient in the CCHP system
η_h	Heating coefficient of the waste heat boiler
η_c	Cooling coefficient of the absorption chiller
η_b	Efficiency of the gas boiler

ACKNOWLEDGEMENTS

The past year has gone quickly and seemed still too short. In this year's study and life, I have learned a lot, not only in the professional aspect, but also in the ability to face difficulties, be down-to-earth, and solve problems step by step. As it gets closer to graduation, I feel a lot of mixed emotions in my heart. On the one hand, I am happy, and on the other hand, there remains some sadness. The so-called joy is because I am about to graduate, and set foot on a new starting point on the road of life. However, it is bittersweet because the people and things I experienced in this year will always be in my mind. There are many people to be thankful for.

First of all, I would like to thank my advisor Professor Lingfeng Wang, as well as Dr. Zhaoxi Liu and Dr. Li Ma, for giving me selfless guidance throughout my graduate career. In the process of writing my thesis, they gave me a lot of help and advice, so that I could complete my thesis more smoothly. Their academic attitudes toward research inspire me to keep studying in whole life. At the same time, their academic guidance has enabled me to accept new knowledge more systematically, improve my level of scientific research, and improve my ability overall. Here I pay my best respects to them.

Secondly, I would like to thank my roommates and classmates. Throughout this year, we cultivated a family-like relationship. The laughter in the lab often made me forget the pressure of research. Being with them made me more optimistic and helped me get through stressful situations. Especially, I am grateful to my friend Yanan Zhang for her selfless help in the process of writing

my thesis. She helped me to create ideas and solve the problems. I hope that my friends will do well in the future.

I am also grateful to the financial support for this project. This work was supported in part by the National Science Foundation Industry/University Cooperative Research Center on Grid-connected Advanced Power Electronic Systems (GRAPES) under Awards GR-17-14 and GR-18-02.

Finally, I would like to thank Dr. David Yu and Dr. Guangwu Xu for their time and effort in serving on my defense committee and their valuable comments and suggestions.

1 Introduction

1.1 Background

Energy is an important material basis for the survival and development of human society. With the continuous development of the social economy, the consumption of energy in human life is increasing. However, traditional fossil fuels such as coal and oil are gradually depleted, and environmental problems such as global warming and air pollution are increasing at the same time. Vigorously developing and utilizing distributed renewable energy and changing the structure of high-carbon energy consumption have become important parts of sustainable development of human society.

At present, the world's energy structure has been profoundly adjusted, and a new round of energy revolution is on the rise. However, the planning and operation of energy systems is still limited to a single energy system at this stage. The comprehensive management and coordinated operation of multiple energy sources can fully utilize their complementary advantages, promote renewable energy consumption, and achieve optimal resource allocation and efficient use of energy [1]. Therefore, improving energy efficiency, exploring new energy sources, realizing large-scale development of renewable energy, researching on collaborative planning and operation of various energy sources, and finally building a unified social integrated energy system will become an inevitable choice of a clean, safe and efficient modern energy system.

In this regard, governments have vigorously carried out researches and practices related to multi-energy systems. In 2001, the US Department of Energy proposed an integrated energy system (IES) development plan to promote multi-energy comprehensive planning, increase the proportion of renewable energy supply, and enhance the economy and reliability of energy system

operation [2-3]. In 2003, Switzerland established the "Vision of Future Energy Networks" research project to optimize the system structure and operation strategy by modeling multi-energy systems to achieve synergies such as multi-energy interactive benefit and energy cascade utilization [4]. In 2008, Germany began implementing "E-energy" program in various areas to promote the use of Internet technologies in enterprises and regions to build complex energy regulation systems [5]. In recent years, China has also actively promoted the development of "interactive network +" smart energy development, and proposed to accelerate the construction of intelligent systems for energy production and consumption, multi-energy collaborative integrated energy networks, and related information and communication facilities.

With the deepening of research on multi-energy systems, the quantity of key components is increasing, and the degree of energy coupling is further deepened, and the load is increasingly diversified. It has been widely discussed that how to model the energy production, conversion, distribution and storage in multi-energy systems while retaining the main characteristics of each energy sources and satisfying the energy balance constraints. Among the many energy system modeling methods, the concept of "energy hub (EH)" proposed by the Eidgenössische Technische Hochschule Zürich (ETH Zürich) is a typical representative [6-7], which has received extensive attention from academia and industry. An energy hub is an input-output dual-port model for describing energy supply, load demand, network switching, and coupling relationships in a multi-energy system. It is a powerful concept of how to acquire, convert, and distribute energy sources in a specific region [8]. The coupling matrix can be used to express the coupling relationships of conversion, distribution, and storage among multiple energy sources. It is widely used in multi-energy system planning and operation analysis [9].

There are certain limitations to consider only the transmission and conversion equipment for basic energy hub modeling in multi-energy systems. With the popularization of energy storage systems [10], electric vehicles [11], demand response [12], and combined cooling heating and power (CCHP) systems, it is of great significance to fully consider the promotion of these elements into energy hub modeling. The distributed CCHP system will be an important method to meet the increasing energy demand. Its abatement cost is much lower than that of traditional fossil energy supply while generating same amount of power. The energy utilization efficiency of CCHP system is also greatly improved compared with the traditional coal-fired power plants. From the operator's point of view, they can also get good benefits and reduce the loss of power supply. The CCHP system is an important energy conversion equipment and an important way to improve energy efficiency and reduce carbon emissions at this stage.

In summary, it will greatly improve the energy efficiency and operational safety of the energy system as well as reduce the cost of society to construct a multi-energy system that fully considers the coupling and complementary relationships of various forms of energy. Based on the existing researches, in order to improve the renewable energy utilization rate and economic benefits, this thesis comprehensively considers the buying-selling price structure of gas and electricity, and establishes an optimization model for energy hub scheduling to coordinate energy supply of solar power and natural gas. At the same time, considering the factors such as the EV driving patterns and the uncertainty of PV output, a mathematical model of energy hub with energy storage systems and CCHP system is constructed. The optimization target of the energy hub model is to minimize the gas cost and electricity cost. This comprehensive research of energy hub has certain impetus

to the improvement of energy hub modeling, and it is of great significance for improving the environmental, economic and social benefits of energy utilization.

1.2 Literature review

1.2.1 CCHP system modeling

There have been a lot of achievements in the establishment of CCHP system optimization scheduling model. The main optimization objectives include: the minimum cost target from the user's point of view [13-14], the minimum carbon emission target from the power grid's point of view [15], or the multi-objective optimization [16].

In [17], based on the difference of load characteristics between office system and living residential system, an energy coupling-based CCHP system optimization model was established to optimize the ratio of office building area to residential area. Literature [18] used thermodynamic methods to calculate the cost and loss of each component of the system, in order to optimize the optimal equipment configuration and operation scheduling of distributed CCHP system. Literature [19] constructed an optimization model that considered fuel utilization, operating costs and environmental benefits at the same time, and used genetic algorithm to solve the nonlinear model. Literature [20] mainly considered the energy utilization rate and operating costs, and compared the traditional distribution system with the CHP system. In [21], a hybrid real-time operation strategy was proposed based on different evaluation systems, and the operation mode of the CCHP system equipment was determined according to different load conditions. Some researches of CCHP system optimal operation also considered the uncertainty of renewable energy and load: In [22], a linear regression model and a time series model were combined to propose a new statistical

prediction algorithm to predict electrical load and cooling load. Literature [23] coordinated the capacity of CHP system, gas boiler, absorption chiller and energy storage equipment. The analysis results of the actual system showed that the proposed method can reduce costs more effectively compared with each energy system planned separately.

1.2.2 Optimization operation of energy hubs

The energy hub describes various coupling relationships between transmission, conversion and storage of various forms of energy, and plays an important role in the planning and operation of multi-energy systems. Scholars have carried out detailed researches on energy hubs [24], including the modeling of energy hubs and its application in the planning and operation of multi-energy systems. In [25], the optimization goal is to minimize the annual cost and the energy efficiency, and the genetic algorithm was used to optimize the capacity of each device in the CCHP system. Literature [26] established a two-layer optimization planning and designing model. The outer model determined the construction and installation capacity of the energy conversion equipment and energy storage unit in the energy hubs, and the inner layer model optimized the typical operating conditions. In [27], based on the statistical analysis of power generation, heating technology, energy demand and traffic model in several countries in the European Union, simplified models of energy hubs in different countries were constructed. Literature [28] constructed an energy hub model considering CHP, renewable energy, energy storage and demand response.

The optimal operation of energy hub describes that the multi-energy system reaches the goal of minimum operation cost, minimum carbon emission or maximum renewable energy consumption by optimizing the distribution and transformation of various forms of energy while meeting the requirements of corresponding energy demand and equipment operation constraints.

At present, according to the number of research targets, the energy hub optimization operation can be divided into two types: single energy hub optimization operation and coordinated optimization operation of multiple energy hubs [29, 30, 35, 36]. There have been a lot of literatures on the optimization of single energy hub operations. Literature [31] established a residential energy hub optimization model that considered the full use of real-time electricity prices and optimal management of energy storage units. The simulation results showed that it can effectively reduce the cost by 60% and the carbon emissions by 25%. In [32], based on the graph theory, the corresponding efficiency matrix of the energy hub with a small-scale CCHP system was derived. Based on this, a nonlinear optimization model with CCHP considering time-varying energy price is established. Literature [33] studied the multi-energy system with hydrogen storage, fully considered the constraints of power grid and gas network, and constructed an optimization model aiming at maximizing the daily profit of power plants. Literature [34] comprehensively considered the uncertainty of wind power output, electricity price and demand, as well as the energy procurement cost and corresponding procurement risk, and constructed the energy hub optimization operation objective function.

The energy hub has a high degree of flexibility in modeling the multi-energy system, and the entire system is often modeled and analyzed using multiple energy hubs [35-36]. The goals of multi energy hub coordinated operation optimization are diverse, including the largest amount of renewable energy consumption and the lowest total cost. Literature [37] constructed a general optimization framework for a complex multi-energy system with multiple energy hubs based on energy exchange with other surrounding energy hubs. Literature [38] considered the bidding price of electricity, gas, etc., the cost of failure risk and other factors, and analyzed the energy hub of a distribution network from the perspective of power retailers. Literature [39] briefly analyzed an

electric and gas system with three energy hubs. The simulation results of case study showed that such a system is beneficial to stabilize voltage amplitude and reduce network loss, as well as reduce the marginal cost of electricity price and increase the marginal cost of natural gas.

At present, the researches on the optimization operation of a single energy hub mainly focus on the treatment of external factors such as load, distributed energy and various uncertainties contained in the energy hub. The lack of research on the internal unit operating characteristics of the energy hub may result in a waste of crew resources.

2 System Model Establishment

2.1 Energy hub model

2.1.1 Energy hub structure

An energy hub (EH) is a multi-input/multi-output unit which could generate, convert and store different forms of energy. This unit has the capability of assisting energy management and optimization by combining and coupling multiple energy carriers. It is a concept with a high degree of abstraction that can describe a multi-energy system model of any size, as small to independent residential users, commercial buildings, factories [30], and as large to countries.

The system architecture of the EH in this thesis is shown in Fig. 1. This is a typical example of an energy hub configuration, and it consists of a transformer, a combined cooling, heating and power generation (CCHP) system, a natural gas boiler, and a refrigerator/air conditioner. There are two kinds of energy inputs: electricity and natural gas, in which the electricity comes from both power grid and the PV components. And the outputs consist of three forms: electricity, heat and cool. These energy carriers are processed within the hub, in order to supply the electric loads and thermal loads.

There are mainly three parts contained in the proposed energy hub: energy generation part, energy conversion part and energy consumption part. Energy generation part shows the energy resources of the EH, such as power grid, photovoltaic components. Energy conversion part displays the transformation relationships between the input and output forms of energy in the EH. It's the core part of EH structure. Energy consumption part includes various load demands and energy storage systems (ESS). Electric vehicles play the role as transferable electric load, which

is distinguished from regular electric load of community consumers. And the thermal load is divided into heating load and cooling load.

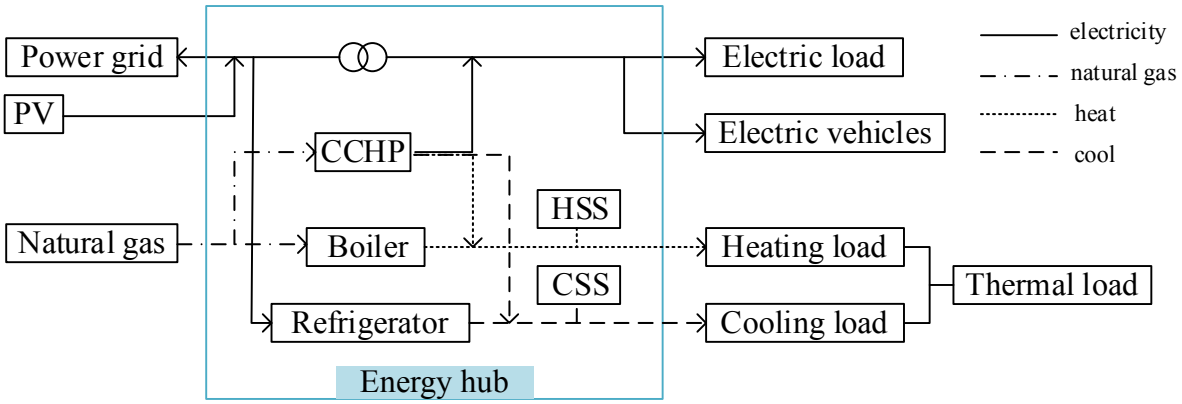

Fig. 1 The system structure of the EH

2.1.2 Energy generation part

From the energy hub structure, the energy input vector P comprises electricity, PV components and natural gas

$$P = \begin{pmatrix} P_{el} \\ P_{pv} \\ P_{gas} \end{pmatrix} \tag{2-1}$$

The P_{el} is the real-time buying amount of electricity from power grid, and it is positive when the grid is supplying the electricity loads, while it is negative when the grid is fed from the energy hub. The P_{gas} is the amount of natural gas from gas market. According to energy policies, they are supposed to be in a bounded range (2-2) and (2-3).

$$-P_{el}^{\max} \le P_{el} \le P_{el}^{\max} \tag{2-2}$$

$$0 \le P_{gas} \le P_{gas}^{\max} \tag{2-3}$$

As for P_{pv}, a photovoltaic component is a device that converts solar energy into electrical energy. Compared with traditional power generation systems, PV modules use solar power to generate electricity. There is no energy depletion problem. Also, there is no primary energy acquisition cost and no noise and pollutant emissions. However, its equipment investment is too high and power generation efficiency is low. The output power (kW) expression for solar irradiance I (kW/m^2) and time period of t has been shown to be obtainable by the following equation

$$P_{pv}(t) = \eta A_{pv} I(t)\left[1 - 0.005(T_a(t) - 25)\right] \tag{2-4}$$

where η is the conversion efficiency of the solar cell array (%); A_{pv} is the array area (m^2); I is the solar radiation (kW/m); and T_a is the ambient temperature (℃).

2.1.3 Energy conversion part

Within the energy hub, energy is converted to various forms for meeting the load demand at the hub output ports. An energy converter converts one kind of energy into another, or affects the energy carrier in quantity and quality. The mathematical model of the converter can be established by using the input-output correlation. In this case, the main characteristic of a component is its efficiency. Fig. 2 demonstrates an expression of single-input single-output converter.

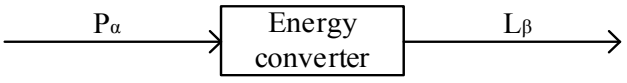

Fig. 2 Single-input single-output converter

It can be observed in Fig. 2 that input energy carrier P_α is converted into L_β by the single-input single-output energy converter. Obviously, the input flow and the output flow are related. The energy transferred from an input hub port to an output hub port can be expressed as

$$L_\beta = \mathrm{C}_{\alpha\beta} P_\alpha \tag{2-5}$$

where P_α and L_β denote energy input and output, respectively. And $C_{\alpha\beta}$ is the coupling factor, demonstrating the coupling rate between input and output.

As mentioned earlier, for a single-input single-output converter, the coupling coefficient corresponds to the efficiency of the converter. The efficiency of the converter can be a variable as a function of the operating point.

Generally, consider a typical energy hub with various energy carriers α, β, ..., γ, in which the energy at input and output ports are represented by vector $P = [P_\alpha, P_\beta, ..., P_\gamma]$ and vector $L = [L_\alpha, L_\beta, ..., L_\gamma]$, respectively. Then energy conversion with a multi-input and multi-output converter can be demonstrated as

$$\underbrace{\begin{pmatrix} L_\alpha \\ L_\beta \\ \vdots \\ L_\gamma \end{pmatrix}}_{L} = \underbrace{\begin{pmatrix} C_{\alpha\alpha} & C_{\beta\alpha} & \cdots & C_{\gamma\alpha} \\ C_{\alpha\beta} & C_{\beta\beta} & \cdots & C_{\gamma\beta} \\ \vdots & \vdots & \ddots & \vdots \\ C_{\alpha\gamma} & C_{\beta\gamma} & \cdots & C_{\gamma\gamma} \end{pmatrix}}_{C} \underbrace{\begin{pmatrix} P_\alpha \\ P_\beta \\ \vdots \\ P_\gamma \end{pmatrix}}_{P} \tag{2-6}$$

The matrix C is a forward coupling matrix describing the transformation of energy from input to output. The elements of the coupling matrix are coupling coefficients, which represent the converter efficiency and internal topology of energy hub. As long as the converter efficiency remains constant, the coupling matrix represents a linear transformation from the input energy to the output. In Fig. 1, the coupling matrix represents four converter devices: 1) transformer; 2) CCHP system; 3) natural gas boiler and 4) refrigerator/air conditioner.

The transformer is a device which is common in the power system to transform voltage from one degree to another, the input and output of it are all electricity. The CCHP system is fed by natural gas and is able to generate electricity, heat and cool, whose inner structure will be introduced later. The gas boiler converses natural gas into heat to meet the heating demand together with CCHP system. And the refrigerator is a cooling-generation device fed by electricity which helps the CCHP system to meet the cooling demand. Heating energy and cooling energy are stored in heating storage system (HSS) and cooling storage system (CSS) at a given time, respectively, to be used later.

2.1.4 Energy consumption part

The load demand vector L comprises electricity load and thermal load. Electricity load comes from customers and electric vehicles, and thermal load contains heating load and cooling load.

$$L = \begin{pmatrix} L_{el} \\ L_{EV} \\ L_h \\ L_c \end{pmatrix} \tag{2-7}$$

where L_{el}, L_h, L_c respectively represents regular electricity load, heating load, and cooling load of customers in community; L_{EV} represents total charging amount of several EVs, which is decided by the EV driving patterns.

Energy storage equipment can decouple the generation and consumption of energy to coordinate the time imbalance between “source and load”, realize energy transfer across time domain, and have the effect of suppressing fluctuations in renewable energy [40]. Electrical energy storage and thermal energy storage are typical energy storage devices in energy hubs, frequently-

used models for them are as follows:

a. Electric energy storage

Electric energy storage equipment are divided into energy type and power type, which can reduce the peak-to-valley difference of power load and reduce operating costs. Energy-type electrical energy storage devices such as batteries are generally used in energy hubs, and their output characteristics are characterized by average output power. In our model, we have electric vehicles as transferable loads which can also reduce the peak-to-valley difference in load demand and play the role as batteries as well as vehicle-to-grid (V2G) devices.

b. Thermal energy storage equipment

There are often mismatches between the peak period and valley period of the thermoelectric load. When the electrical load is high and the thermal load is low, there is often heat waste, which leads to the phenomenon that the energy hub is unable to fully exert its performance. Conversely, when the electric load is low and the thermal load is high, excessive power may be uneconomical. The use of thermal energy storage equipment can realize the transfer of thermal energy, slow down the dilemma of the mismatch of heat-to-electric ratio between the energy hub and the load, and promote the efficient and economic operation of the energy hub.

2.1.5 Energy conservation functions

The energy hub is a system that comprehensively utilizes various forms of energy such as electricity and natural gas, and can enhance the efficiency of producing and utilizing energy. In the proposed energy hub model, the PV components and the power grid supply electricity to part

of the EH's electrical load; the remaining part of the electrical load is supplied by the electricity output of the CCHP system; the heating load is first provided by the waste heat boiler in the CCHP system, and the insufficient part is supplemented by the gas boiler; the cooling load is supplied by the absorption chiller in the CCHP system and the refrigerator which is fed by electricity; the EH purchases electricity from the power grid or sells electricity to the power grid based on the tariff structure of electricity and natural gas. The renewable energy sources used in this model include solar energy.

The most important constraints in the operation of energy hub is meeting electrical, cooling and heating load demands considered in equations (2-8) to (2-11).

$$\eta_{tr} \cdot (P_{el} + P_{pv} - P_r) + L^{e}_{cchp} = L_{el} + L^{ch}_{ev} \tag{2-8}$$

$$P_{gas} = P^{cchp}_{gas} + P^{b}_{gas} \tag{2-9}$$

$$L_h = L_b + L^{h}_{cchp} \tag{2-10}$$

$$L_c = L_r + L^{c}_{cchp} \tag{2-11}$$

where η_{tr} represents the efficiency of the transformer; L^{ch}_{ev} represents the charging amount of electricity per hour per EV (minus value means EV is discharged at the moment).

In each optimization operation cycle, the energy hub meets the electricity demand through the electricity generation by gas boiler, the output of photovoltaic components, the purchase of electricity from the power grid, and the discharge of EVs. When the electricity price is low, the purchasing electricity from the power grid and the PV power output remaining after meeting the electricity energy demand of the energy hub will be stored in the EVs, and preferentially supply the energy hub for consumption in the next period. The EV load is equivalent to increasing the electrical load, as well as improving the system's ability to accept renewable energy, and can also

enhance the role of the electric-gas coupling link in the system and the system's energy supply stability. When the price of electricity is high, the profit of EV discharging is greater than the cost of electricity consumption, the remaining electric energy in the EVs can be sold to the grid after the energy demand of the energy hub is met to constitute the feedback energy, so that the electric energy flows in both directions between the large power grid and the energy hub, increasing the system operation flexibility. Thermal energy is only transmitted in the heating network inside the energy hub.

2.2 CCHP system

2.2.1 CCHP system and its characteristics

Natural gas-fueled power plants, such as gas turbines, gas-fired internal combustion engines, Stirling engines, fuel cells, etc., while generating electricity, the waste heat of the exhaust is recycled for heating or driving air-conditioning refrigeration devices, such as absorption chillers or dehumidification devices. Such a cogeneration system that uses natural gas as fuel and has the functions of power generation, heating, and cooling (or dehumidification) is called Combined Cooling, Heating and Power (CCHP) system. Auxiliary heating and cooling equipment in CCHP system include gas turbines, waste heat boilers, and absorption chillers.

The following is a brief introduction to the performance characteristics of the CCHP system in terms of energy utilization, environmental impact, and economic performance relative to conventional energy systems.

a. Energy utilization

The CCHP system converts the high-temperature heat energy of the fuel into electric energy first, and the low-temperature heat energy is used for heating or cooling. This energy utilization

mode realizes the cascade utilization of energy. Compared with direct heating or cooling after combustion of fuel, it creates favorable conditions for energy conservation.

It can be obtained from previous researches that compared with conventional energy supply systems, the natural gas CCHP system can save energy by up to 25%. Therefore, compared with conventional systems, the CCHP system generally has energy-saving advantages under heating conditions. However, in many cooling conditions, the CCHP system does not have the advantage of energy saving. Therefore, the CCHP system cannot be blindly promoted, and its healthy development on a rational path should be regulated.

b. Environmental impact

The advantages of natural gas CCHP system in environmental protection are mainly reflected in the use of natural gas which is kinds of clean fuel and the reduction of air pollutant emissions from the cogeneration system.

Since electricity in several countries is mainly derived from coal-fired power generation, the replacement of coal-fired power plants by natural gas combined heat and power supply systems has greatly reduced emissions of SO_2, CO_2, soot, NO_x, and so on. On the other hand, because the energy consumption of the CCHP system is lower than the conventional energy system under appropriate condition, the application of the CCHP system directly leads to the reduction of environmental pollutant emissions. Additionally, the promotion and application of some low pollutant discharge technology in power area such as three-way catalytic technology and pre-mixed lean combustion technology, has greatly reduced the emissions of major natural gas pollutants. However, it should also be noted that for the same heating, electricity and cooling load demand, the amount of natural gas consumed by the CCHP system is greater than that of

conventional electric refrigerator, gas boiler and external electricity purchase, so the CCHP system emits more of the local pollutants.

c. Economic performance

The evaluation of the economic efficiency of a system depends mainly on two aspects, namely initial investment and operating costs. To meet the same heating, electricity and cooling load demand, from the initial investment point of view, compared with the conventional system, the CCHP system mainly increases the power generation equipment, that is, the cogeneration power plant, so the initial investment of the system is higher than the conventional system. From the perspective of operating costs, on the one hand, due to the advantages of energy utilization efficiency of CCHP system, especially in heating conditions, there is a possibility of low fuel cost; on the other hand, compared with conventional grid power supply, the CCHP system power supply eliminates the cost of long-distance transmission of the regional power grid and the transmission and distribution of the urban power grid, thus replacing the expensive grid power transmission, and its economic efficiency is reflected in the power generation price. Therefore, although the initial investment of the CCHP system is relatively high, in a suitable condition, due to the reduction of the operating cost, it still has an economic advantage compared with the conventional power supply system which generates heat and cold electricity separately.

d. Balancing peaks and valleys of energy load

In terms of electricity, with the improvement of people's living standards and the popularity of air conditioners, the summer electric load has increased rapidly, and in many cities, it has surpassed winter and become a seasonal peak load. The sharp increase in summer power load has placed a heavy burden on the urban power grid. Due to the constraints of urban power grid capacity, there are often situations in which power cuts are imposed, which has a serious impact on urban

economic development and citizens' normal life. However, in terms of gas, especially the gas in the northern cities, due to a large proportion of gas are used for heating, the summer is the valley period of gas load, and the winter is the peak period of gas load.

The application of CCHP system in summer has reduced the peak load of urban power while increasing the summer load of natural gas. The reduction of peak load of urban power by CCHP system is reflected in two aspects. On the one hand, the thermal power unit generates electricity; on the other hand, the waste heat recycled refrigeration replaces the conventional electric refrigeration to satisfy the air-conditioning load. This distributed energy system dispersed in the urban load center can effectively alleviate the impact of power peaks on urban power transmission and distribution systems. In summary, the operation of CCHP system in summer is beneficial to balance the peak-to-valley difference between urban power and gas load.

2.2.2 Working principle of the CCHP system

A typical diagram of the CCHP system is shown in Fig. 3. Natural gas-fueled prime movers (internal combustion engines, gas turbines, fuel cells, Stirling engines, etc.) first produce and output electrical energy, while recovering the waste heat from the prime mover in the forms of flue gas, steam, hot water, etc., for heating or cooling. In addition to waste heat boilers (heat exchangers), absorption chillers, dehumidifiers and other equipment that directly use waste heat, in order to increase the stability and reliability of system power supply, heating supply, and cooling supply, electric chillers, gas boilers and energy storage devices are generally required in the whole energy hub system.

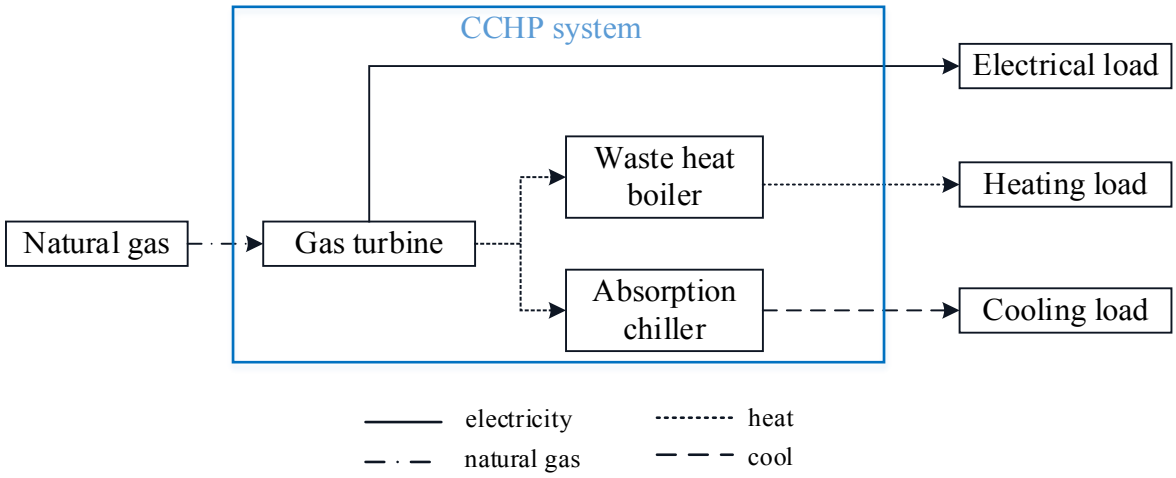

Fig. 3 The principle diagram of CCHP system

Gas turbines can use gaseous fossil energy sources such as natural gas and coal gas as fuel. The gaseous fuel is thoroughly mixed with compressed high-pressure air in the combustion chamber of the gas turbine and burned to produce 1500-2000℃ high-temperature gas. Energy is mediated by high-temperature and high-pressure gas, which causes the impeller of the gas turbine to drive the compressor impeller to generate electricity, or directly supply heat to the waste heat boiler. The waste heat boiler collects the waste heat generated by the turbine, and at the same time, it can extract high-temperature and high-pressure gas directly from the combustion chamber inside the gas turbine according to the dispatching command, to provide heating energy for the load. The absorption chiller uses the thermal energy of the waste heat boiler and the auxiliary boiler as the driving power to provide the users with cooling energy. The wind turbines in the CCHP system are coordinated with the gas turbines and the urban grid to meet the demand for electrical loads of the user side.

Equations (2-8) (2-10) and (2-11) show the relationships between three forms of output of the CCHP system and the energy hub load demands. There are also constraints of efficiencies in the inner structure [41], which is usually applied from the industry point of view by the following relationship

$$P_{gas}^{cchp} = \frac{L_{cchp}^{e}}{\eta_{cchp}} \tag{2-12}$$

$$L_{cchp}^{e} \cdot \frac{1-\eta_{cchp}-\eta_{loss}}{\eta_{cchp}} = \frac{L_{cchp}^{h}}{\eta_{h}} + \frac{L_{cchp}^{c}}{\eta_{c}} \tag{2-13}$$

where η_{cchp} is power generation efficiency of the gas turbine; η_{loss} is heat loss coefficient in the CCHP system; η_h is heating coefficient of the waste heat boiler; η_c is cooling coefficient of the absorption chiller.

Additionally, the CCHP system also follows the feasible region for three outputs which are specified with equations (2-14) and (2-15).

$$0 \le P_{gas}^{cchp} \le P_{gas} \tag{2-14}$$

$$\begin{aligned} L_{cchp}^{e} &\ge 0 \\ L_{cchp}^{h} &\ge 0 \\ L_{cchp}^{c} &\ge 0 \end{aligned} \tag{2-15}$$

Since the fuel of the CCHP system comes from the input natural gas, and the natural gas flows into both CCHP system and the independent gas boiler, the amount of gas injected into the CCHP

system should be definitely less than the total amount of natural gas input from the gas market. From the output point of view, three forms of energy output are required to be non-negativity.

The cost of the CCHP system can be defined as C_{cchp} [42]

$$C_{cchp} = (\frac{p_{gas}}{L}) \cdot (\frac{L^{e}_{cchp}}{\eta_{cchp}}) \tag{2-16}$$

where p_{gas} is the price of natural gas; L is the low heating value of natural gas.

2.3 Boiler and refrigerator

2.3.1 Gas boiler

The natural gas from the gas market enters the gas boiler as a primary energy fuel, and the high-temperature flue gas brought by the combustion is used to drive the generator to produce electric energy.

$$L_b = \eta_b \cdot P^{b}_{gas} \tag{2-17}$$

where η_b is the efficiency of the gas boiler.

Since the fuel of the boiler comes from the input natural gas, and the natural gas flows into both CCHP system and the independent gas boiler, the amount of gas injected into the boiler should be definitely less than the total amount of natural gas bought from the gas market, as indicated in equation (2-18).

$$0 \le P^{b}_{gas} \le P_{gas} \tag{2-18}$$

Additionally, the output of boiler should be within the maximum limitation.

$$0 \le L_b \le L_b^{\max} \tag{2-19}$$

2.3.2 Refrigerator/air-conditioner

The electric refrigerator liquefies the refrigerant gas by mechanical pressurization, and completes the transfer of thermal energy through the characteristic that evaporation of liquid refrigerant requires heat absorption, thereby realizing the conversion of electric energy into cooling energy. From the principle point of view, the electric refrigerator is more efficient than the absorption chiller inside the CCHP system. Therefore, when the electricity price is low, the use of the electric refrigerator can improve the overall operating economy. At the same time, when absorption chiller cannot meet the cooling load demand at the cold load peak period, the electric refrigerator plays an important role in assisting refrigeration. The ratio of the input electricity quantity of the electric refrigerator to the output cooling quantity is called the cooling coefficient, expressed by η_r, which is less affected by the load rate. The working characteristics can be expressed as (2-20) and (2-21):

$$L_r = \eta_r \cdot P_r \tag{2-20}$$

$$0 \le L_r \le L_r^{\max} \tag{2-21}$$

In equation (2-20), L_r and P_r represent the output cooling energy and the amount of electricity consumed by the electric refrigerator during the period *t*, respectively. And $L_r^{\max}$ in equation (2-21) is the maximum limit of refrigerator output.

2.4 Electric vehicles modeling

2.4.1 Model description

With the popularization of electric vehicles, the energy supply infrastructures of them have also been widely promoted. Compared with the conventional long-term charging method, the quick charging method has higher requirements on technology and has a great influence on battery life. The public power station can not only complete the charging demand of the electric vehicles in a short time, but also has the characteristics of economy and quickness. In addition, a large number of batteries in the power station can serve as the role of charging and energy storage devices. When the power supply demands are ensured, the remaining power is fed back to the power grid, and the charging and discharging time periods of the power station can be reasonably controlled to achieve the load translation and the demand response. The effect is equivalent to the transferable load.

As bidirectional and transferable power loads, electric vehicles have definite uncertainties in terms of charging and discharging time and space. Disordered charging and discharging of large-scale electric vehicles will bring huge challenges to the stable operation of power grid. With the advancement of electric vehicles technology, the concept of vehicle-to-grid (V2G) and its feasibility of interacting with the power grid have attracted more and more attention. The electric vehicles obtain electric energy from the power grid as transferable loads, and at the same time they can be used as energy storage devices to transfer electric energy to the power grid to realize two-way exchange of electric energy and information between the electric vehicles and the power grid. The interactive application between them is called V2G [43].

V2G disordered charging mode means that the vehicle owner determines the charging and discharging behavior according to his driving habits. Generally, when the electric vehicle user arrives at the charging station, charging begins, regardless of the influence of the peak-to-valley

time-sharing electricity price, which may increase the peak load of the power demand in the system. Aiming at the random access problem of large-scale electric vehicles, under the premise of satisfying the needs of users, reasonable means can be used to guide and dispatch the charging and discharging behavior of users, effectively disperse the load of electric vehicles, and provide sufficient power for users to meet the power demand. It is necessary to reduce the operating cost of the power grid as much as possible, and reduce the adverse impact of the uncertainties of electric vehicles on the power grid.

Generally speaking, a complete simulation cycle is a one-day (24 hours) time period. Therefore, in the process of establishing a model to describe EV driving patterns, simulation cycle starts at midnight, and the coverage time in each simulation is not necessarily 24 hours but determined by the arrival and departure time of the EVs. The establishment of the scenario set for EV itineraries is based on the statistical analysis of EV electricity consumption. In the rolling horizon optimization, the battery SOC scheduling is assigned for every horizon T during the whole simulation cycle to achieve the minimum running cost for the system.

2.4.2 EV model establishment

For a single electric vehicle, the factors that determine its charging load are mainly the charging power and the charging time interval, which depend on the user's driving pattern. The driving characteristics of the owner have an important influence on the state of charge of the electric vehicle battery. The determination of the charging period interval is mainly related to the charging start time and the end time. For the parking lot of a public building, the time period from the arrival time of the vehicle to the departure time of the vehicle is the chargeable time period.

However, the time to start charging is random, and it is affected by uncertain factors such as the expected value of the state of charge. In order to clarify the initial state of charge, charging availability coefficient (whether it can be charged) and expected state of charge for each electric vehicle, we established a data set to represent the load demand of the electric vehicles.

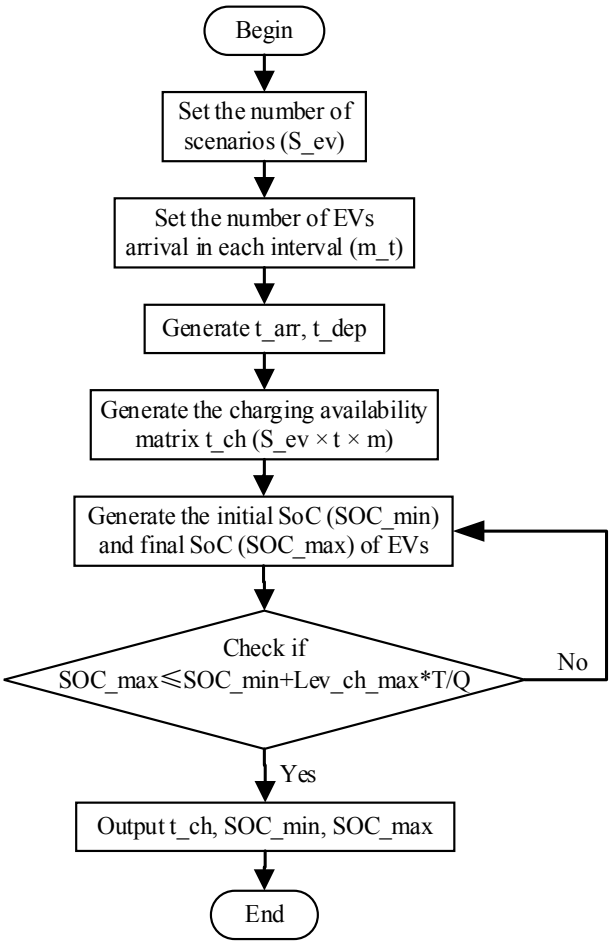

Fig. 4 The flow chart of EV model establishment

From the flow chart, we can clearly describe the process of generation of EV scenarios which mainly contain the charging availability matrix t_{ch}, the initial SOC SOC_{e0} and the expected SOC $SOC_e^{\max}$.

The battery charging power (L_{ev}^{ch}) is assumed to be positive while it is being charged and negative during discharging. Based on the definition of L_{ev}^{ch}, L_{ev}^{m} represents the charging amount of electricity per hour for all EVs when the EV amount is m. The state of charge (SOC) level of each EV is calculated with the cumulated charging energy and the initial SOC. The time-related SOC is defined as follows:

$$SOC(t) = SOC_0 + \frac{\sum_{i=1}^{t} L_{ev}^{ch}(i)}{Q} \tag{2-22}$$

Also, the battery charging and discharging power limits are set to avoid overcharge and over discharge, that is, the effective capacity is less than the full capacity of battery Q. The SOC limit constraint (2-23), and the EV charging energy limit constraint (2-24) need to be satisfied:

$$0 \le SOC \le 1 \tag{2-23}$$

$$-L_{ev}^{ch\max} \cdot t_{ch} \le L_{ev}^{ch} \le L_{ev}^{ch\max} \cdot t_{ch} \tag{2-24}$$

In each time interval, the SOC levels of the EV batteries are within the specified range. For the charging energy limit constraint (2-24), the EV charging energy is constrained by the maximum power limitation and the expected EV charging availability coefficient. Parameter $L_{ev}^{ch\max}$ is the maximum charging power for per EV every hour. The EV charging availability coefficient t_{ch} shows the expected status of the EV at time period t, and the matrix using binary variables 0/1 to describe whether the EV is being charged or not, as indicated in equation (2-25).

$$t_{ch} = \begin{cases} 1, & t_{arr} \le t \le t_{dep} \\ 0, & \text{otherwise} \end{cases} \tag{2-25}$$

Vehicle-to-grid (V2G) technology is considered in this energy hub and EVs are regarded as not only electricity demands but also power supplies. Therefore, the charging energy during a

specific hour can be negative as constraint (2-24) indicates. For simplicity, it is assumed that the energy hub is served for a public building, so the available periods for each EV charging scheduling is the period between the arrival time and the departure time. The duration of charging is related to the battery capacity, the charging power, the initial SOC of the battery before charging, and the expected SOC when the electric vehicle departures. For the convenience of analysis, regardless of changes in charging and discharging efficiency, battery temperature, etc., the relationship between SOC and charging load is shown as follows. Then the energy transfer of each EV *i* over the total scheduling time *t* satisfy equation (2-26).

$$L_{ev}^{t} = SOC_{e}^{\max} \cdot Q - SOC_{e0} \cdot Q \tag{2-26}$$

where L_{ev}^{t} represents the charging amount of electricity per EV for 24 hours.

During the scheduling time period, the SOC of each EV should reach the expected SOC level $SOC_{e}^{\max}$. SOC_{e0} is the state of charge of each EV before charging, and the initial SOC of the batteries are different due to the difference in user's traveling and charging habits. For a single electric vehicle, the expected SOC value $SOC_{e}^{\max}$ of the battery can be obtained from the daily mileage.

2.5 Heating storage system and cooling storage system

As mentioned above, there are often mismatches between the peak period and valley period of the thermoelectric load. When the electrical load is high and the thermal load is low, there is often heat waste, which leads to the phenomenon that the energy hub unable to fully exert its performance. Conversely, when the electric load is low and the thermal load is high, excessive

power may be uneconomical. The use of thermal energy storage devices can realize the transfer of thermal energy, slow down the dilemma of the mismatch of heat-to-electric ratio between the cogeneration system and the load, and promote the efficient and economic operation of the energy hub.

Since we divide thermal load into heating load and cooling load in the customer side, correspondingly, we need heating storage system (HSS) and cooling storage system (CSS) in the energy hub. The energy storage system can be placed at the input port of the system, which is equivalent to the correction of the input matrix *P* as (2-1) indicates. It can also be at the output port of the system, which is equivalent to the correction of the input matrix *L* as (2-7) indicates. First, the energy entering or leaving the energy storage system should be limited by constraints (2-27) and (2-28).

$$L_h + S_h^{ch} = L_{cchp}^h + L_b \tag{2-27}$$

$$L_c + S_c^{ch} = L_{cchp}^c + L_r \tag{2-28}$$

where S_h^{ch} and S_c^{ch} is the storage energy entering or leaving the energy storage system each hour. S_h^{ch} is limited by a maximum power $S_h^{\max}$, that is, $-S_{ch}^{\max} \le S_h^{ch} \le S_{ch}^{\max}$. So as S_c^{ch}.

$S_h(t)$ is defined as the amount of heating energy injected into storage system till time *t*, which can be expressed as follows:

$$S_h(t) = \sum_{i=1}^{t} S_h^{ch}(t) \tag{2-29}$$

And the SOC of HSS can be defined and limited as follows:

$$SOC_h = SOC_0 + \frac{S_h}{Q_h} \tag{2-30}$$

$$0 \le SOC_h \le 1 \tag{2-31}$$

where Q_h represents heat storage capacity of HSS.

For the CSS, we have a series of constraints similar as HSS, shown as constraints (2-32) to (2-34).

$$S_c(t) = \sum_{i=1}^{t} S_c^{ch}(t) \tag{2-32}$$

$$SOC_c = SOC_0 + \frac{S_c}{Q_c} \tag{2-33}$$

$$0 \le SOC_c \le 1 \tag{2-34}$$

3 Real-Time Rolling Horizon Optimization

3.1 Rolling horizon optimization strategy

Rolling horizon optimization strategy is a strategy which combines prediction, time domain rolling optimization and feedforward-feedback together. It is a specific manifestation of the principle of rolling optimization in predictive control. The main difference between rolling optimization and traditional optimal control is that the system with rolling horizon optimization is not optimized throughout the entire process, nor is it only optimized once, but rather a rolling process in a limited time horizon. In a dynamic uncertain environment, it is meaningless to consider optimization in a long period of time, and because of the unpredictability of environmental changes, optimization needs to be repeated. Therefore, the idea of rolling optimization is particularly targeted for dynamic environments.

Rolling window technology is at the heart of rolling horizon optimization. When applying the rolling window technology for dynamic scheduling, first we need to define three windows: the completion window, the scheduling processing window and the waiting window, as shown in Figure 5. The waiting window stores all the tasks waiting to be scheduled, and the completion window stores all the tasks that have been processed. The scheduling processing window refers to the optimized time horizon window in the rolling optimization principle. It selects a certain number of tasks from the waiting window and place them in the scheduling processing window. After scheduling, these scheduled tasks are processed according to the scheduling results. The

scheduling processing window includes the processing task set and the unprocessed task set. The processing task set is a scheduled task set that is already in processing. The unprocessed task set is a set of tasks that have been scheduled but have not yet started processing.

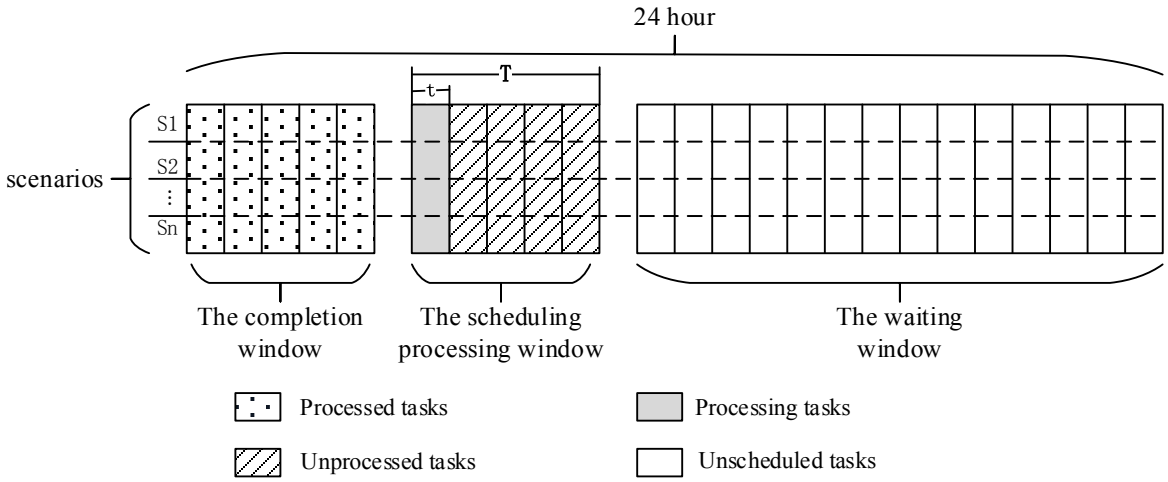

Fig. 5 The relationship between rolling window and task sets

The basic principle of rolling horizon optimization is: at each moment, based on the current state information, the control vector in the finite time domain is solved, and the first control variable is applied to the controlled object as the actual control variable at the next moment. By analogy, the above process is repeated at the next moment, and the new state information is used to solve the control variables to form an iterative optimization process. As shown in Fig. 5, T is the prediction duration, the control variables of the (T-1) steps are predicted in the future at time t, and the prediction variable at time t is selected as the actual control variable. Iterative optimizations are performed in combination with the control constraints and the rolling horizon.

Rolling horizon optimization method is a model-based and optimization-based control, which can track changes of the system, continuously push the scrolling of the optimization set in time, apply the scheduling optimization algorithm to solve the scheduling sub-problem, and achieve global optimization by continuously optimizing local optimizations.

3.2 Objective function

The optimization problem is widely applied to the optimization decision in the power system. The optimization model can be divided into single-objective optimization and multi-objective optimization. Single-objective optimization generally determines the maximum or minimum value of the objective function. The properties of the objective function in the model can be divided into two types: benefit function and cost function. However, as far as the same optimization model is concerned, the attributes of different objective functions of decision maker will also change. Therefore, the classification of benefit and cost types is also relative. The research in this thesis only describes the attributes of functions from a single decision-making perspective.

If the optimization model targets the minimum of the objective function, the function is called the cost function. In the eyes of decision maker, the smaller the value of the cost function, the better. Cost function is the most common type of functions in the power system, such as the production cost of the generator units in the optimal power distribution problem, the system network loss in the reactive power optimal allocation problem, and the pollutant emissions in the environmental protection dispatch problem.

If the maximum value of the objective function is the target of the optimization model, the function is called the benefit function. In the opinion of the decision maker, the larger the value of the benefit function, the better. The benefit functions in the power system mainly include system revenue, rate of return on investment, energy use efficiency and safety margin.

Based on the description above, we use cost function below as the objective function:

$$\min Z = p_{el} \cdot P_{el} + (\frac{p_{gas}}{L}) \cdot P_{gas} \tag{3-1}$$

The cost function consists of two parts. The electricity buying price and the gas cost for both CCHP system and boiler. Where p_{el} and p_{gas} are the price of electricity and natural gas; P_{el} and P_{gas} are the consumed amount of electricity and natural gas; L is the low heating value of natural gas.

3.3 Case study

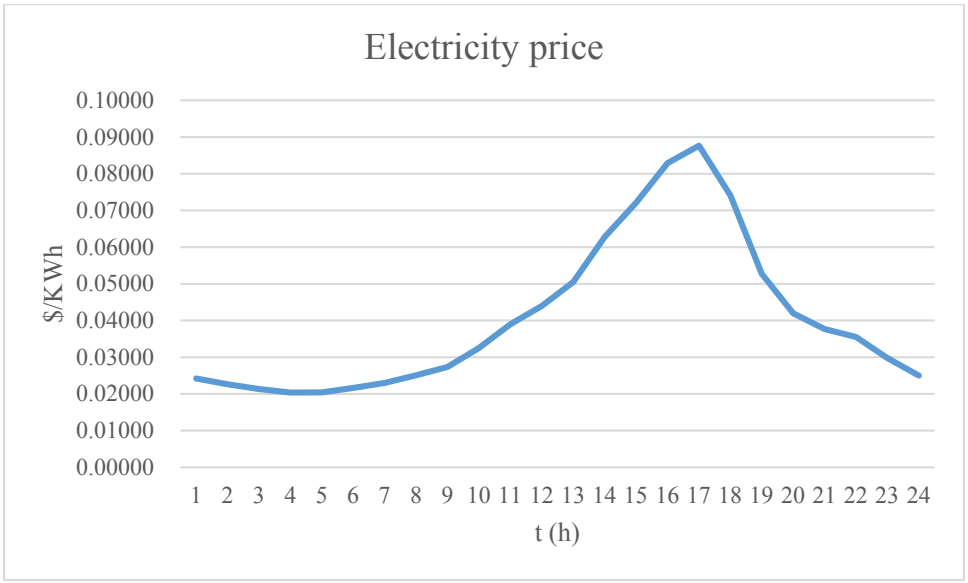

Fig. 6 The hourly electricity price on a regular day

For case study, we choose the 24-hour hourly electricity price on a regular day to demonstrate the peak-to-valley characteristic of the electricity market. Following is simulation results of energy hub scheduling in day-ahead market.

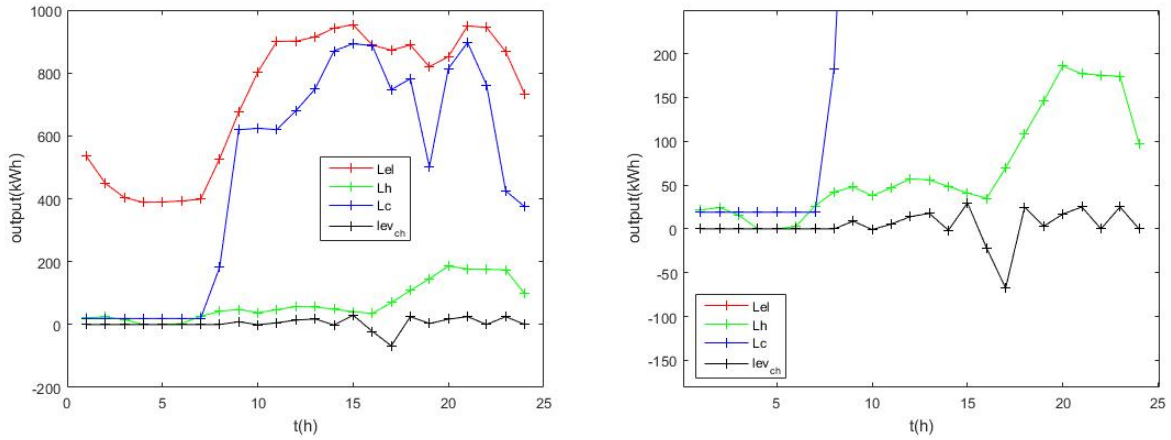

Fig. 7 The simulation results of output energy in day-ahead scheduling

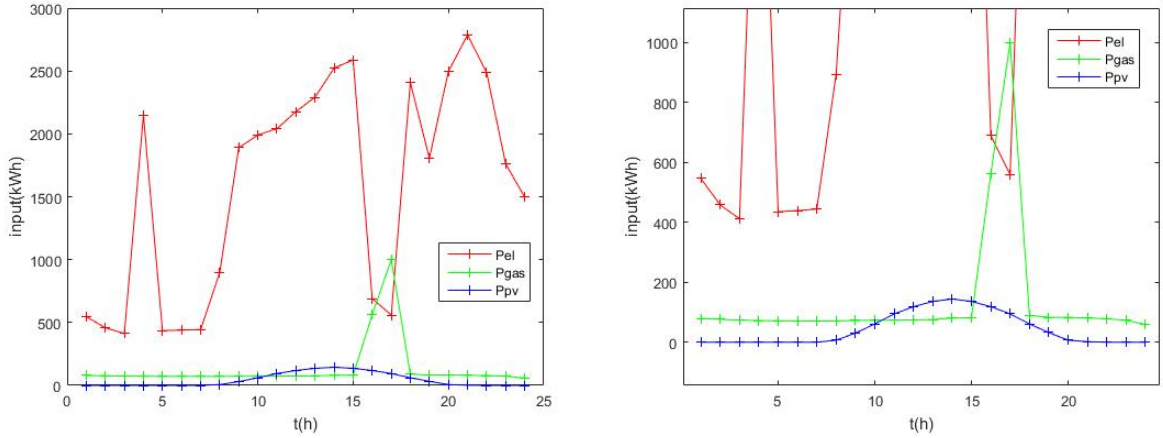

Fig. 8 The simulation results of input energy in day-ahead scheduling

It can be seen from Fig. 8 that the gas purchase curve of day-ahead scheduling is absolutely lower than the electricity purchase curve during most time of the day. And the EV charging curve in Fig. 7 is very sharp. That's because in the day-ahead 24-hour scheduling, the energy is purchased for a whole day's consumption, therefore the energy hub will definitely buy energy more than

needed to ensure the amount can fully meet the load demand in the following day. Only when the time comes to 15-18, during which the electricity price is relatively high, the gas purchase can be more than the electricity purchase. However, this kind of scheduling will result in a large amount of energy loss and it is contrary to our target. Due to the unreasonable results of day-ahead market in scheduling the proposed energy hub model, real-time rolling horizon optimization is applied to shows its superiority with comparison.

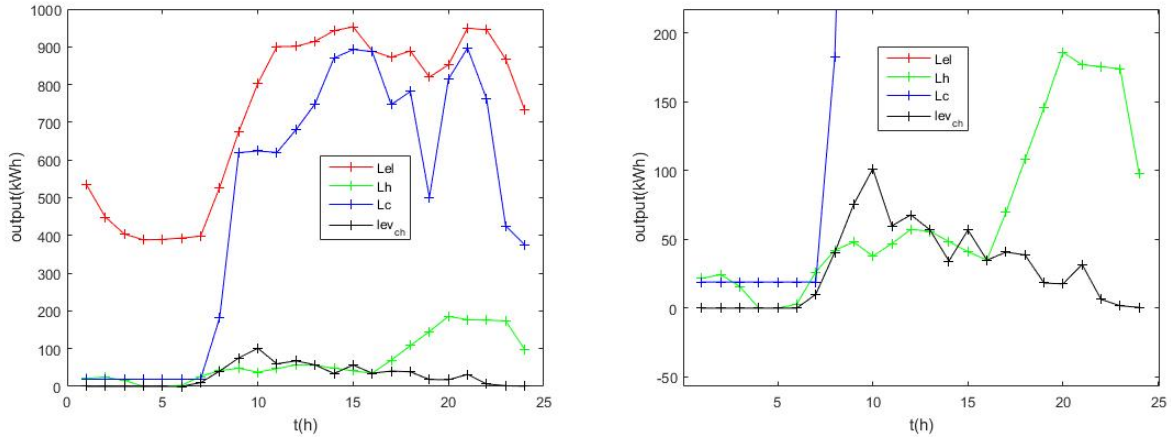

Fig. 9 The simulation results of output energy in real-time rolling horizon scheduling

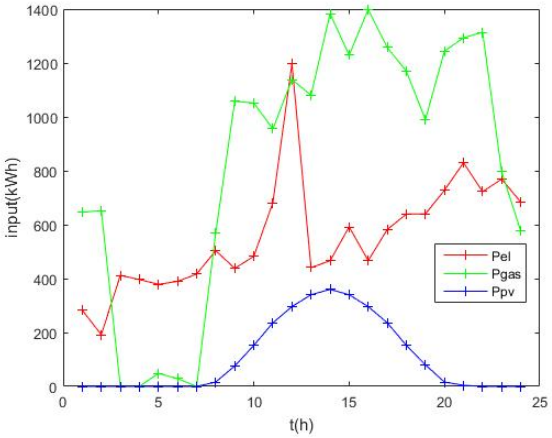

Fig. 10 The simulation results of input energy in real-time rolling horizon scheduling

In real-time rolling horizon scheduling, the optimization principle ensured that the result is optimized each moment, so it avoids energy waste caused by overbuying energy.

However, due to the randomness of the driving patterns, it is still very difficult to perfectly predict the driving consumption and the charging availability of the EVs one day in advance. As a result, there may not have global optimal solutions is the stochastic scheduling of energy hub with EVs. Chance constrained programming is a direct and efficient tool to handle such a predicament. The idea of chance constrained models is to hedge the risk of uncertainty for a big probability and drop the extreme case with a very low probability. It is appropriate to be applied on the different types of uncertainties in the model.

4 Chance Constrained Model for Stochastic Scheduling

4.1 Description of chance constrained programming

Chance constrained programming (CCP) is an important branch of uncertain programming, mainly for the case where the constraint contains a random variable and the decision is made before the realization of the random variable is observed. The chance constrained programming can ensure that the probability that the inequality constraint is satisfied is greater than or equal to a given confidence interval, and the requirement is guaranteed in the form of probability. The decision is allowed to dissatisfy the constraint to a certain extent.

In the engineering field, due to the random nature of the uncertain variable y, it is difficult to obtain a deterministic optimal solution before the implementation of y. However, in the actual optimization decision process, due to the need of scheduling, appropriate optimization decisions must be made before implementation of the random variable. Therefore, the chance constrained programming method that obtains the optimal decision under certain probability can solve the overlap problem well.

If a random variable is included only in the constraint, the generalized chance constrained programming mathematical model can be described as:

$$\begin{cases} \min f(x) \\ s.t.\ \ P_{\mathrm{r}}\{g_i(x,\xi) \le 0, i = 1,2,\cdots,m\} \ge \alpha_i \\ x \in X \subset R^n \end{cases} \tag{4-1}$$

where x represents the n-dimension decision vectors; $f(x)$ is the optimal objective function; $P_{\mathrm{r}}\{\bullet\}$ is the probability of event $\{\bullet\}$ occurring; m is the number of chance constraints; ξ represents the random vector of the probability density function; $g_i(x,\xi) \le 0$ is stochastic constraint function; α_i is the confidence interval required for the establishment of the i th constraint, which is generally given in advance. $P_{\mathrm{r}}\{g_i(x,\xi) \le 0, i = 1,2,\cdots,m\} \ge \alpha_i$ means that the probability that the i th constraint is satisfied should be at least α_i; X represents the feasible region of the decision variable x.

Equation (4-1) indicates that each constraint is independent of each other. If the constraints are not independent of each other, they are represented by the joint chance constrained programming. The joint chance constrained programming is performed on the condition that the objective function and the constraints are all probabilistic constrained. If there is $\alpha_i \ne \alpha_j (j = 1,\cdots,i-1,i+1,\cdots,m)$, that is, there is a difference in the confidence level of each inequality constraints, then the programming is called hybrid chance constrained programming, as shown in equation (4-2).

$$\begin{cases} \min f(x) \\ s.t.\ P_{\mathrm{r}}\{g_i(x,\xi) \le 0, i = 1,2,\cdots,m\} \ge \alpha \\ x \in X \subset R^n \end{cases} \tag{4-2}$$

where α is the confidence interval required for the constraints to be satisfied.

Chance constrained programming can also be generalized to chance-constrained multi-objective programming with the following expression,

$$\begin{cases} \min y = [f_1(x), \ldots, f_M(x)] \\ s.t.\ \ P_r\{g_i(x,\xi) \le 0, i = 1,2,\cdots,m\} \ge \alpha \\ x \in X \subset R^n \end{cases} \tag{4-3}$$

where y is the optimal objective function vector; M is the number of objective functions.

If the objective function that is expected to be minimized also contains a random variable, then equation (4-2) is improved to the following form,

$$\begin{cases} \min \overline{f} \\ s.t.\ \ P_r\left\{f(x,\xi) \le \overline{f}\right\} \ge \beta \\ \qquad P_r\{g_i(x,\xi) \le 0, i = 1,2,\cdots,m\} \ge \alpha \\ x \in X \subset R^n \end{cases} \tag{4-4}$$

where β is the confidence interval required for the optimal objective function which is given in advance; $\overline{f}$ is the minimum value of the objective function when the confidence level is β.

4.2 Solutions of chance constrained programming

Chance constrained programming is an important branch of stochastic programming. Because of its uncertainty, it can't be solved directly. The common solution methods are introduced below. There are three common methods of simplification: 1) transforming chance constrained constraints into deterministic constraints [44]; 2) using scenario analysis methods to generate multiple determined scenarios to finally obtain expectations [45]; and 3) applying intelligent optimization algorithms based on stochastic simulation [46-47].

The traditional method for solving the chance constrained programming is to convert the chance constraints into deterministic constraints according to the given confidence level, and then use the traditional optimization method to solve. Independent chance constraints are more easily to be transformed into deterministic constraints, and the concept of quantile is often used to convert chance constraints to deterministic constraints in form. The key point and difficulty in transforming the chance constraints into deterministic constraints lies in the fast solution of cumulative distribution function (CDF) of the joint variables and its inverse function. In [44], Ozturk et al. used the load output as the uncertainty variable, and used the multivariate normal distribution random variables to express the load. The chance constraint is that the probability, that the power generation output of all time periods was greater than or equal to the load, is not lower than the confidence interval. The multi-time interval constraint was transformed into a time-independent probability constraint, and then the probability constraint of each time period was transformed into a deterministic inequality constraint, and finally the inequality represented by the upper quantile corresponding to the loss-of-load probability was obtained.

The principles of using scenario analysis and intelligent algorithms to solve the chance constrained programming are similar. The stochastic simulation techniques such as Monte Carlo Simulation are used to generate a large number of deterministic scenarios. Each scenario is determined and can be solved by traditional optimization algorithms. When the total number of scenarios is sufficient, the ratio of the number of scenarios satisfying the chance constraint to the

total number of scenarios in the optimization result approximates the probability that the chance constraint holds. Use Monte Carlo simulation to verify whether the chance constraint holds, consider the chance constraint

$$P_{\mathrm{r}}\left\{g_i(x,\xi) \le 0, i = 1,2,\cdots,m\right\} \ge \alpha \tag{4-5}$$

where $\xi = (\xi_1, \xi_2, ..., \xi_d)$ represents the *d*-dimension random vector, each random variable has a known probability distribution. First, *N* independent random vectors $\xi_1, \xi_2, ..., \xi_N$ are generated based on the probability distribution $\Phi(\xi)$. Let N' of the *N* trials satisfy the formula

$$g_i(x,\xi_i) \le 0, i = 1,2,\cdots,N \tag{4-6}$$

That is, N' is the number of random variables which satisfy the constraints among the generated random variables. According to the Law of Large Numbers, the probability N'/N can be used to estimate the probability that the formula (4-6) holds. Therefore, the chance constraint (4-5) holds if and only if $N'/N \ge \alpha$. The larger the total number of generated scenarios is, the closer the estimated probability is to the probability that the actual chance constraint can be satisfied. However, if the total number of scenarios is too large, the amount of calculation will increase. Choosing an appropriate total number of scenarios and using scenario reduction can improve the efficiency of random simulation. In [46], the genetic algorithm based on Monte-Carlo stochastic simulation was used to solve the chance constrained programming and the chance constrained multi-objective programming.

4.3 Chance constrained programming for proposed energy hub

The initial state of charge SOC_{e0}, the expected state of charge $SOC_e^{\max}$ and the charging availability t_{ch} are stochastic parameters dependent on the driving patterns of the EV. To simplify, the minimum and maximum limits of SOC are set to 0 and 1 as indicated in constraint (2-23). What's more, from constraints (2-22) and (2-26), the expected state of charge $SOC_e^{\max}$ is decided by the initial state of charge SOC_{e0}, Therefore, the $SOC_e^{\max}$ does not have much influence on the simulation results, the randomness of the driving patterns lies in constraints (2-24), which can be reformulated in a chance constrained framework as,

$$P_{\mathrm{r}}\left\{\begin{array}{l} L_{ev}^{ch} \geq -L_{ev}^{ch\max} \cdot t_{ch} \\ L_{ev}^{ch} \leq L_{ev}^{ch\max} \cdot t_{ch} \end{array}\right\} \geq \alpha \tag{4-7}$$

A realization of the possible driving pattern is noted by the parameters t_{ch} associated with the probability π_k. A binary variable z_k is introduced for each driving pattern realization and the probabilistic constraint (4-7) can be reformulated as (4-8) to (4-10).

$$L_{ev}^{ch} \geq -L_{ev}^{ch\max} \cdot t_{ch} + L_{ev}^{ch\max} \cdot z_k \tag{4-8}$$

$$L_{ev}^{ch} \leq L_{ev}^{ch\max} \cdot t_{ch} + L_{ev}^{ch\max} \cdot z_k \tag{4-9}$$

$$\sum(\pi_k \cdot z_k) \leq 1 - \alpha \tag{4-10}$$

When the binary variable $z_k = 0$, constraints (4-8) and (4-9) have a similar form as (2-24) and the constraints are guaranteed for the driving pattern realization *k*. When the binary variable $z_k = 1$, constraints (4-8) and (4-9) can be reformulated to (4-11) and (4-12).

$$L_{ev}^{ch} \geq -L_{ev}^{ch\max} \cdot (t_{ch} - 1) \tag{4-11}$$

$$L_{ev}^{ch} \leq L_{ev}^{ch\max} \cdot (t_{ch} + 1) \tag{4-12}$$

Constraints (4-11) and (4-12) are always satisfied in the feasible region of the optimization problem ($-L_{ev}^{ch\max} \leq L_{ev}^{ch} \leq L_{ev}^{ch\max}$) given a reasonable initial SOC condition. Therefore, the constraints of the driving patterns realization *k* will not affect the solution of the optimization when $z_k = 1$. In constraint (4-10), π_k is the probability of the realization *k* of the possible driving patterns. The constraint (4-10) is equivalent to the probabilistic constraint as shown in (4-13) and therefore the original probabilistic constraint (4-7) can be satisfied.

$$\sum \pi_k \cdot (1 - z_k) \geq \alpha \tag{4-13}$$

5 Case Study

5.1 Related data

The structure of proposed energy hub has been illustrated in Fig. 1, which shows that the chosen energy hub is connected to the electricity and natural gas infrastructures at the input side and provides electricity, heat and cool at the output-side ports. The test data of three forms of load demand for the energy hub are shown in Fig. 11. To simulate the model, real-time data of a public building has been considered as a case study. The energy hub consists of a transformer, a boiler, a refrigerator, a HSS and a CSS, as well as the essential part, a CCHP system. The CCHP system produces heating and cooling energy and power simultaneously when it is committed. The features of the energy hub elements have been listed in Table 1.

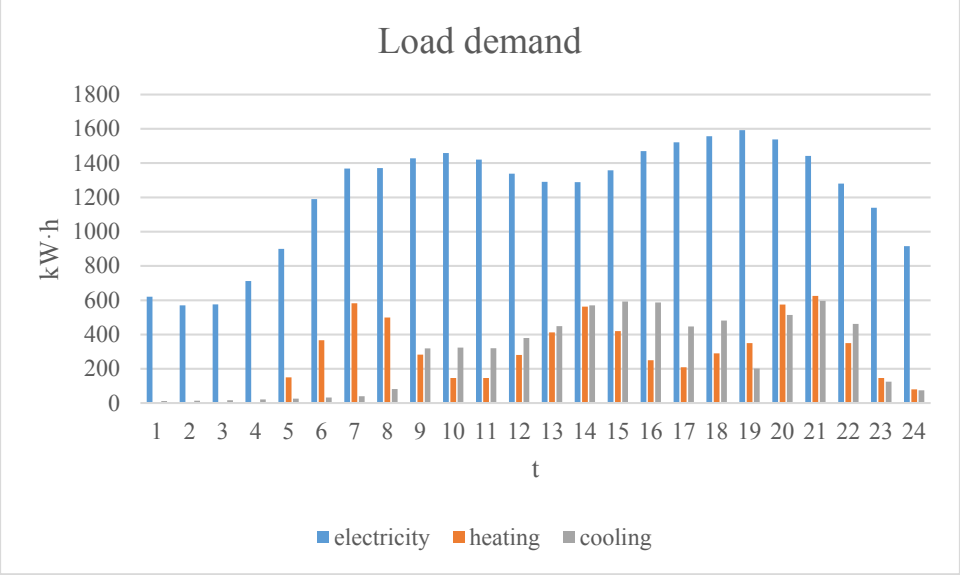

Fig. 11 Electricity, heating and cooling demand

Table 1 Devices parameters inside EH

Input ports	$-6000\text{kW} \leq P_{el} \leq 6000\ \text{kW}$ $0 \leq P_{gas} \leq 8000\text{kW}$
CCHP system	$\eta_{cchp} = 0.4 \quad \eta_{loss} = 0.05$ $\eta_h = 0.8 \quad \eta_c = 1.2$
Transformer	$\eta_{tr} = 0.98$
Boiler	$\eta_b = 0.85,\ 0 \leq L_b \leq 1000\text{kW}$
Refrigerator	$\eta_r = 0.50,\ 0 \leq L_r \leq 1000\text{kW}$
Heating storage system	$Q_h = 1000\ \text{kW}\cdot\text{h}$ $0 \leq S_h^{ch} \leq 150\ \text{kW}\cdot\text{h}$
Cooling storage system	$Q_c = 1000\ \text{kW}\cdot\text{h}$ $0 \leq S_c^{ch} \leq 150\ \text{kW}\cdot\text{h}$

The output power of PV have been shown in Fig. 7. In this case study, multiple scenarios have been considered for sun's irradiance and load. Scenarios can be obtained by sampling from a continuous probability distribution; however, it is possible to establish a discrete probabilities table by the experience [48]. The PV output used in the case study is the dataset generated from the five scenarios with equal probabilities.

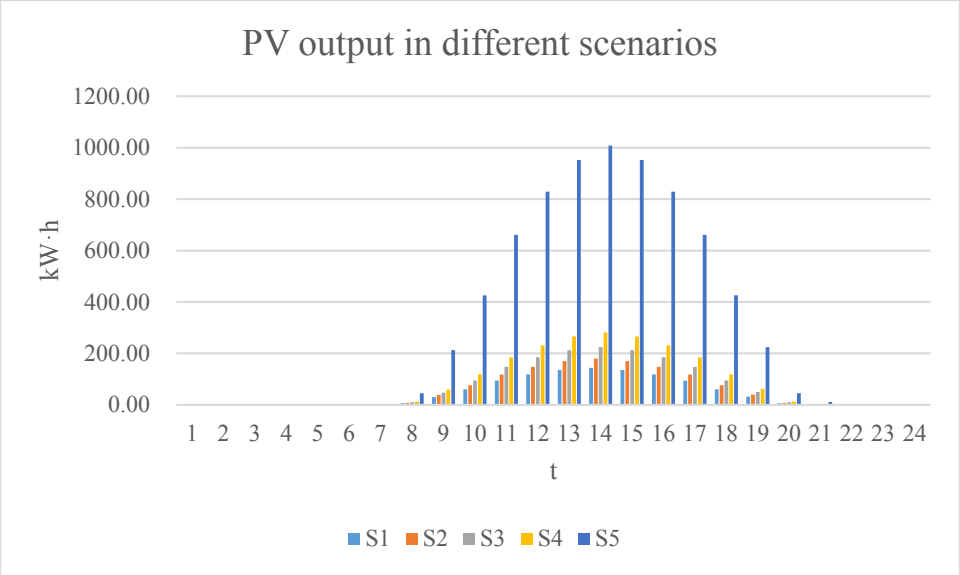

Fig. 12 The output power of PV

The energy hub can purchase electricity from the power grid, at a time-varying price of electricity market. There are two common trading modes in the electricity market: day-ahead energy market and real-time energy market. The day-ahead energy market lets market participants commit to buy or sell wholesale electricity one day before the operating day, to help avoid price volatility. This market produces one financial settlement. The real-time energy market lets market participants buy and sell wholesale electricity during the course of the operating day. The real-time energy market balances the differences between day-ahead commitments and the actual real-time demand for and production of electricity. The real-time energy market produces a separate, second financial settlement. It establishes the real-time locational marginal price (LMP) that is either paid or charged to participants in the day-ahead energy market for demand or generation that deviates from the day-ahead commitments. Table 2 and Fig. 6 represents the hourly electricity price based on the power market on a regular day. As it can be seen, electricity prices vary at different hourly time periods.

Table 2 Hourly price of open energy market in a typical day ($/kWh)

Time	1	2	3	4	5	6	7	8
Price	0.02419	0.02263	0.02132	0.02038	0.02040	0.02164	0.02299	0.02509
Time	9	10	11	12	13	14	15	16
Price	0.02736	0.03254	0.03899	0.04398	0.05048	0.06277	0.07214	0.08289
Time	17	18	19	20	21	22	23	24
Price	0.08767	0.07410	0.05273	0.04197	0.03766	0.03550	0.02974	0.02498

In many countries, natural gas tariffs for different load sectors (including domestic, commercial and industrial) are different. Typically, the industrial tariffs in the United States are cheaper than domestic tariffs. Contrary to the electricity market, the real-time market for purchasing natural gas has not been taken into account. Due to the possibility of bilateral contracts with some options for a certain period, in the presented study, a fixed price of 0.088 $/kWh has been considered for natural gas during the scheduling day.

5.2 Simulation results and analysis

As mentioned before, the chance constrained programming mainly limits the constraints of EV charging behavior, and the randomness of EVs are caused by their different driving patterns. In the case study, we set 600 EVs with different driving patterns and they are divided into 30 scenarios with different probabilities.

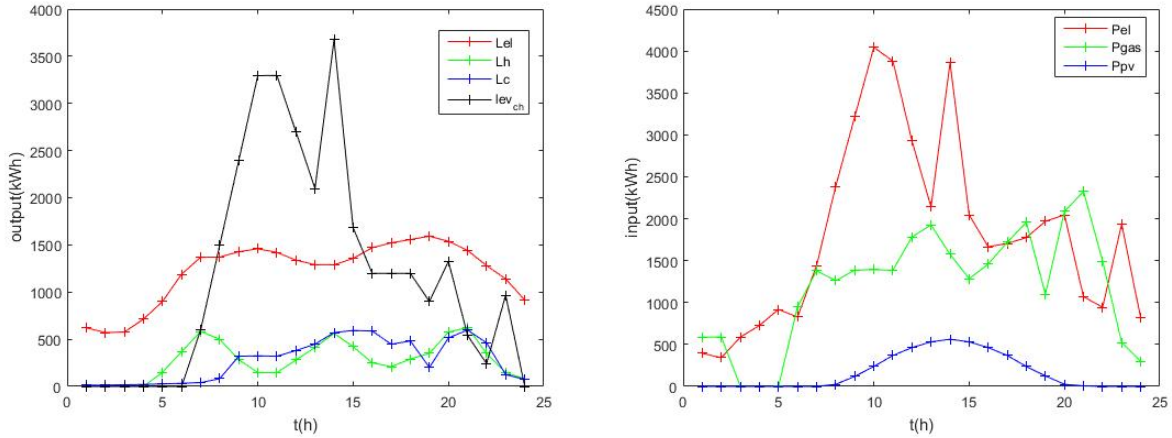

Fig. 13 The simulation results without chance constrained programming

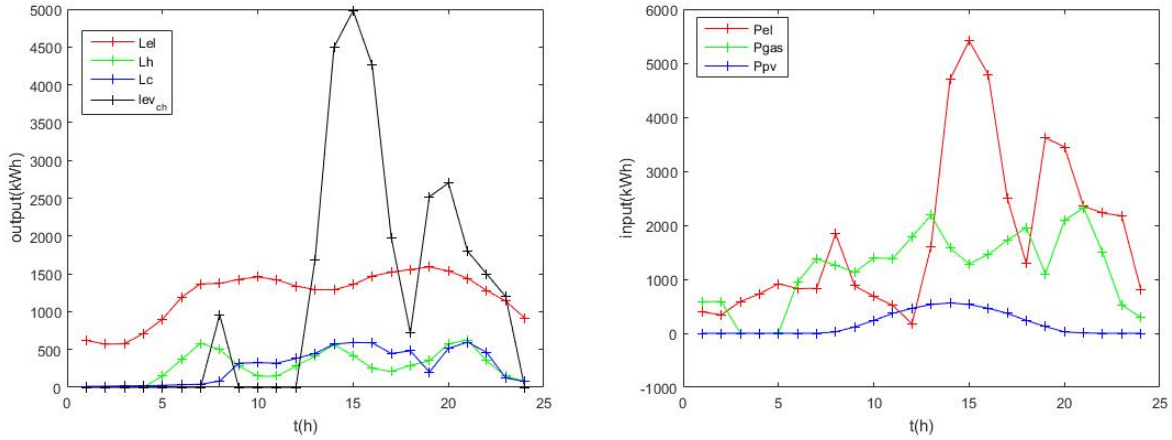

Fig. 14 The simulation results with chance constrained programming

The confidence coefficient α in the established chance constrained programming is 95%. Under the confidence coefficient, the energy cost of EH scheduling model without CCP is \$2804.24/day, and the energy cost of EH scheduling model with CCP is \$2327.03/day. It shows that CCP apparently reduces the energy cost of EH optimization scheduling. The confidence coefficient α allows the decision to dissatisfy the constraint to a certain extent, so some extreme scenarios are discarded by the CCP in the optimization process, which leads to a more economic scheduling of the EH.

Although our objective function is to minimize the energy cost of the whole energy hub, the chance constrained programming can not only improve the system in the aspect of energy cost. From the differences between Fig. 13 and Fig. 14, it can be seen that the EV charging curve in the simulation results with CCP can better make use of the time-varying PV output.

To clarify this point, we establish another set of case study with higher PV output. We increase the probabilities of some higher PV output scenarios to create a new dataset with higher PV power output.

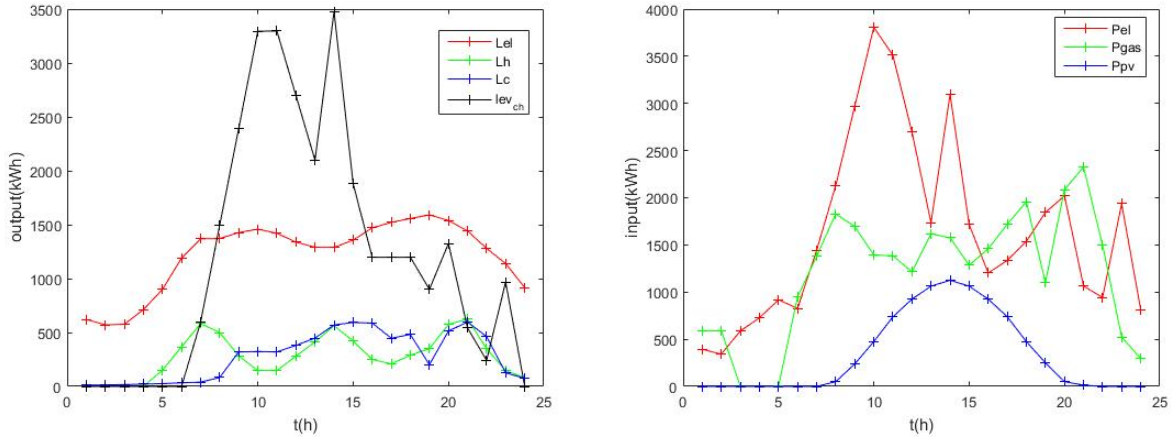

Fig. 15 The higher PV output simulation results without chance constrained programming

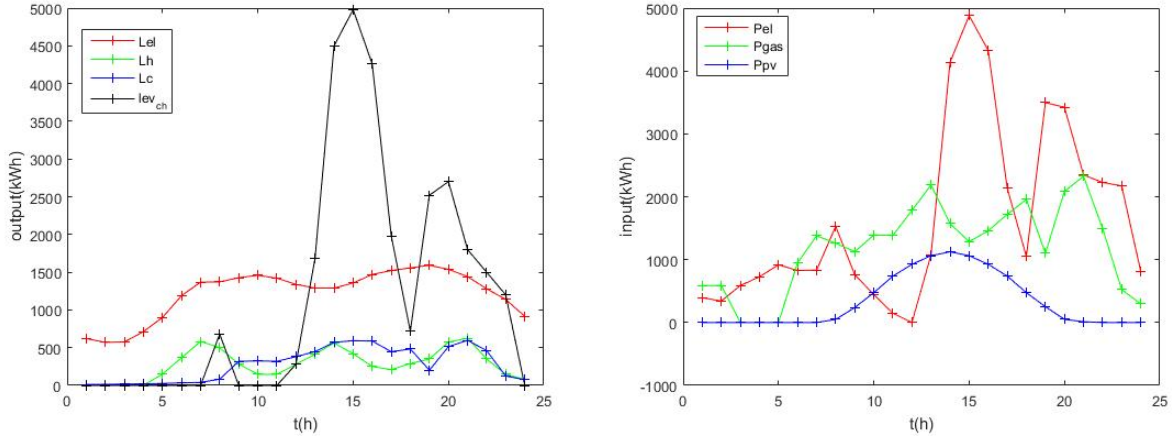

Fig. 16 The higher PV output simulation results with chance constrained programming

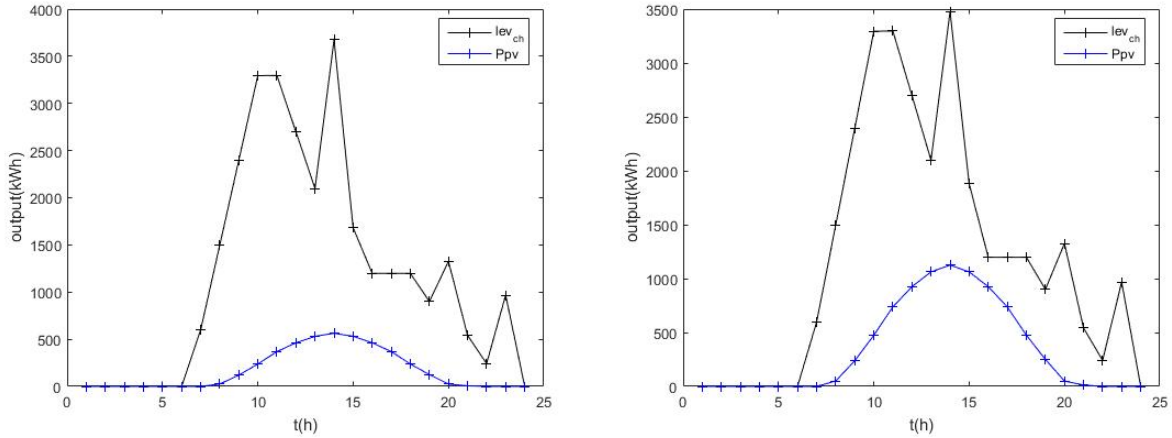

Fig. 17 The comparison of EV charging and PV output curves without chance constrained programming

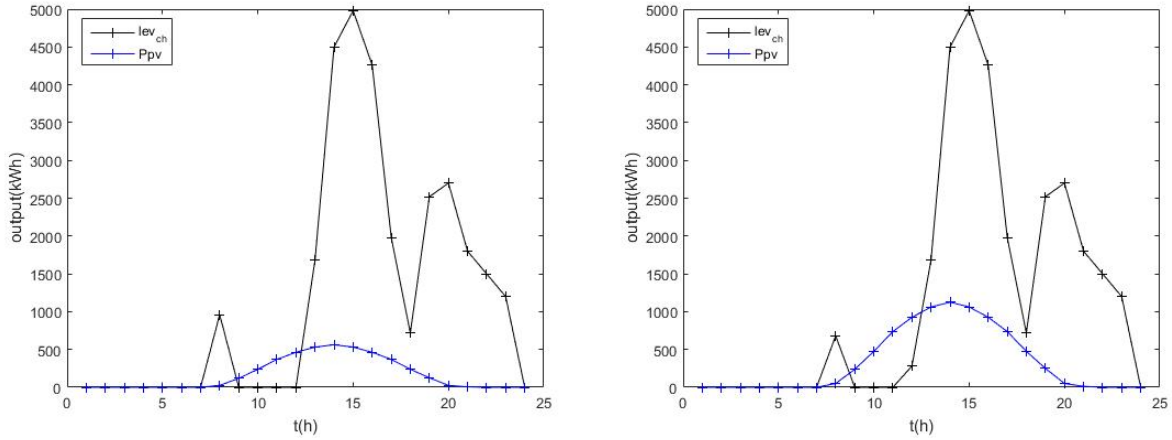

Fig. 18 The comparison of EV charging and PV output curves with chance constrained programming

The EV charging behaviors of EH optimization scheduling with chance constrained programming can make better use of the time period when the PV output is high. In a broad sense, this advantage of CCP can ensure the EH scheduling to better adapt to uncertainty factors, which demonstrates its superiority in energy hub optimization scheduling.

6 Conclusions and Prospects

In the context of the global energy and environmental crisis, researches on the multi-energy system is in full swing. Building a multi-energy system that considers various forms of energy such as electricity, heat, and gas will greatly improve the comprehensive utilization efficiency of the energy system. As an important method for analyzing multi-energy systems, energy hubs modeling cannot only consider the transmission and conversion equipment of multi-energy systems. With the popularization of energy storage, CCHP system and distributed renewable energy integration, and the gradual maturity of V2G technology, it is of great significance to fully consider these elements for the promotion of energy hub models.

6.1 Conclusions

This thesis establishes an energy hub optimization model with CCHP system and combines it with EVs and V2G technology to construct an improved energy hub model. Since the day-ahead electricity market cannot respond to the current system behavior in a timely and effective manner, we use the rolling horizon algorithm to solve the real-time optimization scheduling problem. And the uncertainties of the constructed scenarios of PV output and EV driving patterns may cause the problem to fail to reach the global optimal solution of the model, so we joined chance constrained programming in the optimization. The main results of the thesis and the conclusions are as follows:

(1) Based on the background of a public building, an energy hub model with energy storage systems, PV components and CCHP system is constructed. By the complement of the internal energy flow of the CCHP system, the transformation of electric energy and thermal energy in the energy hub is clarified.

(2) Based on the proposed model, considering the influences of V2G technology and peak-to-valley electricity price on energy storage and consumption, an improved optimization EH model is proposed. The improved optimization model has the function of peak-shaping and valley-filling based on the peak-to-valley time-sharing electricity price. The electricity purchase result and the real-time electricity price curve are strongly correlated.

(3) Taking the minimum energy cost as the optimization function, the rolling horizon optimization of EH is carried out considering the above constraints. The real-time rolling horizon optimization can get more reasonable results than the day-ahead optimization in the energy hub optimization scheduling problem.

(4) The influence of the uncertainty of electric vehicle charging behavior on energy hub scheduling is studied, and the mathematical model of energy hub optimization using chance constrained programming is established. The correlation between the EV charging behavior and the PV output is analyzed.

6.2 Innovation points

(1) An energy hub model which integrated energy storage systems, PV components, CCHP system and EVs is constructed. The model has also considered the influence of V2G technology on energy storage and consumption.

(2) Rolling horizon optimization is carried out on the proposed model to realize a more accurate real-time scheduling of energy hub.

(3) Chance constrained programming is applied in the energy hub scheduling. The influence of the uncertainty of electric vehicle charging behavior on energy hub scheduling is studied.

6.3 Prospects

Although in this thesis some work have been done on the energy hub stochastic scheduling problem, and some achievements have been made, due to the complexity and time limitation, there are still much research work remaining to be carried out. There are the following aspects:

(1) Although the chance constrained programming model can better coordinate the relationship between the diversity of electric vehicle driving patterns and the energy hub scheduling, due to the complexity of the probabilistic problem, the solution efficiency is not high, and the solution efficiency of the algorithm can be further improved;

(2) This thesis focuses on the internal problems of the energy hub, and does not consider the modeling of the power grid and the gas network on the input side. In the future research, reasonable methods can be used to improve the problem, which can make the problem more in line with practical engineering applications;

(3) As a multi-energy system, research on the application of power-to-gas (P2G) technology can be further studied and analyzed, from the aspects of investment planning, operation optimization strategy, responsibility and benefit distribution of coordinated multi-energy systems.

References

[1] P. Alstone, G. Dimitry, and K. Daniel. “Decentralized Energy Systems for Clean Electricity Access.” Nature Climate Change, vol. 5, no. 4, 2015, pp. 305–314.

[2] A. Quelhas, E. Gil, J.D Mccalley, and S.M Ryan. “A Multiperiod Generalized Network Flow Model of the U.S. Integrated Energy System: Part I-Model Description.” IEEE Transactions on Power Systems, vol. 22, no. 2, 2007, pp. 829–836.

[3] A. Quelhas, and J.D Mccalley. “A Multiperiod Generalized Network Flow Model of the U.S. Integrated Energy System: Part II-Simulation Results.” IEEE Transactions on Power Systems, vol. 22, no. 2, 2007, pp. 837–844.

[4] M. Geidl, and G. Andersson, O.B Fosso. “Integrated Modeling and Optimization of Multi-Carrier Energy Systems.” 2007.

[5] T. Krause, G. Andersson, K. Fröhlich, and A. Vaccaro. “Multiple-Energy Carriers: Modeling of Production, Delivery, and Consumption.” Proceedings of the IEEE, vol. 99, no. 1, 2011, pp. 15–27.

[6] T. Krause, F. Kienzle, Y. Liu and G. Andersson, "Modeling interconnected national energy systems using an energy hub approach," 2011 IEEE Trondheim PowerTech, Trondheim, 2011, pp. 1-7.

[7] P. Favre-Perrod, "A vision of future energy networks," 2005 IEEE Power Engineering Society Inaugural Conference and Exposition in Africa, Durban, 2005, pp. 13-17.

[8] S. Da Huo, C. Gu, K. Ma, W. Wei, Y. Xiang, and L. Blond. “Chance-Constrained Optimization for Multienergy Hub Systems in a Smart City.” IEEE Transactions on Industrial Electronics, vol. 66, no. 2, 2019, pp. 1402–1412.

[9] X. Zhang, M. Shahidehpour, Alabdulwahab, and Abusorrah. “Optimal Expansion Planning of Energy Hub With Multiple Energy Infrastructures.” IEEE Transactions on Smart Grid, vol. 6, no. 5, 2015, pp. 2302–2311.

[10] X. Zhang, G. Karady, and Ariaratnam. “Optimal Allocation of CHP-Based Distributed Generation on Urban Energy Distribution Networks.” IEEE Transactions on Sustainable Energy, vol. 5, no. 1, 2014, pp. 246–253.

[11] M. D. Galus and G. Andersson, "Power system considerations of plug-in hybrid electric vehicles based on a multi energy carrier model," 2009 IEEE Power & Energy Society General Meeting, Calgary, AB, 2009, pp. 1-8.

[12] P. Ahčin and M. Šikić, "Simulating demand response and energy storage in energy distribution systems," 2010 International Conference on Power System Technology, Hangzhou, 2010, pp. 1-7.

[13] Hajabdollahi, Ganjehkaviri, and Jaafar. “Assessment of New Operational Strategy in Optimization of CCHP Plant for Different Climates Using Evolutionary Algorithms.” Applied Thermal Engineering, vol. 75, 2015, pp. 468–480.

[14] Hu, and Cho. “A Probability Constrained Multi-Objective Optimization Model for CCHP System Operation Decision Support.” Applied Energy, vol. 116, 2014, pp. 230–242.

[15] Abdollahi, and Sayyaadi. “Application of the Multi-Objective Optimization and Risk Analysis for the Sizing of a Residential Small-Scale CCHP System.” Energy & Buildings, vol. 60, 2013, pp. 330–344.

[16] Sanaye, and Khakpaay. “Simultaneous Use of MRM (Maximum Rectangle Method) and Optimization Methods in Determining Nominal Capacity of Gas Engines in CCHP (Combined Cooling, Heating and Power) Systems.” Energy, vol. 72, 2014, pp. 145–158.

[17] L. Li, et al. “Optimization and Analysis of CCHP System Based on Energy Loads Coupling of Residential and Office Buildings.” Applied Energy, vol. 136, 2014, pp. 206–216.

[18] Ghaebi, Hadi, et al. “Energy, Exergy and Thermoeconomic Analysis of a Combined Cooling, Heating and Power (CCHP) System with Gas Turbine Prime Mover.” International Journal Of Energy Research, vol. 35, no. 8, 2011, pp. 697–709.

[19] Bischi, et al. “A Detailed MILP Optimization Model for Combined Cooling, Heat and Power System Operation Planning.” Energy, vol. 74, no. C, 2014, pp. 12–26.

[20] S. Sanaye, and H. Hajabdollahi. “Thermo-Economic Optimization of Solar CCHP Using Both Genetic and Particle Swarm Algorithms.” Journal Of Solar Energy Engineering-Transactions Of The Asme, vol. 137, no. 1, 2015, pp. 011001/1–011001/11.

[21] Wu, et al. “Multi-Objective Optimal Operation Strategy Study of Micro-CCHP System.” Energy, vol. 48, no. 1, 2012, pp. 472–483.

[22] Han, et al. “Analysis of Combined Cooling, Heating, and Power Systems under a Compromised Electric–Thermal Load Strategy.” Energy & Buildings, vol. 84, 2014, pp. 586–594.

[23] S. Bahrami S, F. Safe. “A financial approach to evaluate an optimized combined cooling, heat and power system.” Energy and Power Engineering, vol. 5, no. 5, 2013, pp. 352-362.

[24] “Intelligent Energy Europe Invites Proposals on Variety of Schemes.” Renewable Energy Report, no. 94, 2005, p. 30.

[25] Jabbari, et al. “Design and Optimization of CCHP System Incorporated into Kraft Process, Using Pinch Analysis with Pressure Drop Consideration.” Applied Thermal Engineering, vol. 61, no. 1, 2013, pp. 88–97.

[26] Guo, et al. “A Two-Stage Optimal Planning and Design Method for Combined Cooling, Heat and Power Microgrid System.” Energy Conversion and Management, vol. 74, no. C, 2013, pp. 433–445.

[27] T. Krause, F. Kienzle, Y. Liu and G. Andersson, “Modeling interconnected national energy systems using an energy hub approach.” 2011 IEEE Trondheim PowerTech, Trondheim, 2011, pp. 1-7.

[28] S. Pazouki, M. Haghifam and J. Olamaei, “Economical scheduling of multi carrier energy systems integrating Renewable, Energy Storage and Demand Response under Energy Hub approach.” 2013 Smart Grid Conference (SGC), Tehran, 2013, pp. 80-84.

[29] Sheikhi, Aras, et al. “Integrated Demand Side Management Game in Smart Energy Hubs.” IEEE Transactions on Smart Grid, vol. 6, no. 2, 2015, pp. 675–683.

[30] X. Tian, and R. Zhao. “Energy Network Flow Model and Optimization Based on Energy Hub for Big Harbor Industrial Park.” Journal of Coastal Research, vol. 73, no. sp1, 2015, pp. 298–303.

[31] S. Le Blond, F. Li and R. Li. “Cost and emission savings from the deployment of variable electricity tariffs and advanced domestic energy hub storage management.” 2014 IEEE PES General Meeting, Harbor, 2014, pp. 1-5.

[32] Chicco, and Mancarella. “Matrix Modelling of Small-Scale Trigeneration Systems and Application to Operational Optimization.” Energy, vol. 34, no. 3, 2009, pp. 261–273.

[33] R. Proietto et al., “Mixed heuristic-non linear optimization of energy management for hydrogen storage-based multi carrier hubs.” 2014 IEEE International Energy Conference (ENERGYCON), Cavtat, 2014, pp. 1019-1026.

[34] J. Hossain, and A. Mahmud. “Energy hub management with intermittent wind power.” Large Scale Renewable Power Generation. Singapore: Springer, 2014. pp. 413-438.

[35] A. Ghasemi, et al. “Introducing a New Framework for Management of Future Distribution Networks Using Potentials of Energy Hubs.” Iranian Conference on Smart Grids, Tehran, 2012, pp. 1–7.

[36] L. Carradore, and R. Turri. “Modeling and Simulation of Multi-Vector Energy Systems.” 2009 IEEE Bucharest PowerTech, Bucharest, 2009, pp. 1–7.

[37] Del Real, A. J, et al. “Optimal Power Dispatch of Energy Networks Including External Power Exchanges.” 2009 European Control Conference (ECC), Budapest, 2009, pp. 3616–3621.

[38] A. Ghasemi, et al. “Introducing a New Framework for Management of Future Distribution Networks Using Potentials of Energy Hubs.” Iranian Conference on Smart Grids, Tehran, 2012, pp. 1–7.

[39] M. Geidl, and G. Andersson. “Optimal Power Flow of Multiple Energy Carriers.” IEEE Transactions on Power Systems, vol. 22, no. 1, 2007, pp. 145–155.

[40] D.J Swider. “Compressed Air Energy Storage in an Electricity System With Significant Wind Power Generation.” IEEE Transactions on Energy Conversion, vol. 22, no. 1, 2007, pp. 95–102.

[41] M. Houwing, R. R. Negenborn, and B. De Schutter, “Demand Response With Micro-CHP Systems,” Proc. IEEE, vol. 99, no. 1, 2011, pp. 200-213.

[42] J. Chen, X. Yang, L. Zhu, and M. Zhang, “Genetic algorithm basedeconomic operation optimization of a combined heat and power microgrid,” Power Sys. Prot. Control., vol. 41, no. 8, 2013, pp. 7-15.

[43] Y. Zhou, G. Xu and M. Chang, "Demand side management for EV charging/discharging behaviours with particle swarm optimization," Proceeding of the 11th World Congress on Intelligent Control and Automation, Shenyang, 2014, pp. 3660-3664.

[44] U.A Ozturk, et al. “A Solution to the Stochastic Unit Commitment Problem Using Chance Constrained Programming.” IEEE Transactions on Power Systems, vol. 19, no. 3, 2004, pp. 1589–1598.

[45] Z. Liu, et al. “Distribution Locational Marginal Pricing for Optimal Electric Vehicle Charging Through Chance Constrained Mixed-Integer Programming.” IEEE Transactions on Smart Grid, vol. 9, no. 2, 2018, pp. 644–654.

[46] R. K. Jana, and Dinesh K. Sharma. “Genetic Algorithm-Based Fuzzy Goal Programming for Class of Chance-Constrained Programming Problems.” International Journal of Computer Mathematics, vol. 87, no. 4, 2010, pp. 733–742.

[47] C. W. Yu, et al. “Optimal Spinning Reserve Capacity Determination Using a Chance-Constrained Programming Approach.” Electric Power Components and Systems, vol. 35, no. 10, 2007, pp. 1131-1143.

[48] A.Y Saber, G. K Venayagamoorthy. “Resource scheduling under uncertainty in a smart grid with renewables and plug-in vehicles.” IEEE Syst. J., vol. 6, no. 1, 2012, pp. 103–109.